Acta Crystallographica Section C
Structural Chemistry
ISSN 2053-2296

The topotactic dehydration of monoclinic $\{[Co(pht)(bpy)(H_2O)_2]\cdot 2H_2O\}_n$ into orthorhombic $[Co(pht)(bpy)(H_2O)_2]_n$ (pht is phthalate and bpy is 4,4′-bipyridine)

Miguel Angel Harvey, Sebastián Suarez, Fabio D. Cukiernik and Ricardo Baggio

Acta Cryst. (2014). C**70**, 978–982

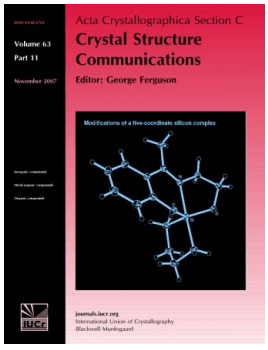

Acta Crystallographica Section C: Structural Chemistry specializes in the rapid dissemination of high-quality detailed studies of novel and challenging crystal and molecular structures of interest in the fields of chemistry, biochemistry, mineralogy, pharmacology, physics and materials science. The unique checking, editing and publishing facilities of the journal ensure the highest standards of structural reliability and presentation, while providing for reports on studies involving special techniques or difficult crystalline materials. Papers go beyond reporting the principal numerical and geometrical data, and may include the discussion of multiple related structures, a detailed description of non-routine structure determinations, placing the structure in an interesting scientific, physical or chemical context, or the discussion of interesting physical properties or modes of association. Reports of difficult or challenging structures, such as cases of twinning, severe disorder, or diffuse solvent regions are welcomed, provided the presented structures are correct and the difficulties and strategies used to treat them are scientifically discussed and properly documented. *Section C* readers have access to an extensive back archive of high-quality structural data.

Acta Crystallographica Section C
Structural Chemistry
ISSN 2053-2296

The topotactic dehydration of monoclinic $\{[Co(pht)(bpy)(H_2O)_2]\cdot 2H_2O\}_n$ into orthorhombic $[Co(pht)(bpy)(H_2O)_2]_n$ (pht is phthalate and bpy is 4,4′-bipyridine)

Miguel Angel Harvey,[a,b]* Sebastián Suarez,[c] Fabio D. Cukiernik[c] and Ricardo Baggio[d]

[a]Universidad Nacional de la Patagonia, Sede Trelew, 9100 Trelew, Chubut, Argentina, [b]CenPat, CONICET, 9120 Puerto Madryn, Chubut, Argentina, [c]Departamento de Química Inorgánica, Analítica y Química, Física/INQUIMAE–CONICET, Facultad de Ciencias Exactas y Naturales, Universidad de Buenos Aires, Buenos Aires, Argentina, and [d]Gerencia de Investigación y Aplicaciones, Centro Atómico Constituyentes, Comisión Nacional de Energía Atómica, Buenos Aires, Argentina
Correspondence e-mail: unharvey@cenpat.edu.ar

Received 7 September 2014
Accepted 11 September 2014

Controlled heating of single crystals of the previously reported [Köferstein & Robl (2007). *Z. Anorg. Allg. Chem.* **633**, 1127–1130] dihydrate $\{[Co(pht)(bpy)(H_2O)_2]\cdot 2H_2O\}_n$, (II) [where pht is phthalate ($C_8H_4O_4$) and bpy is 4,4′-bipyridine ($C_{10}H_8N_2$)], produced a topotactic transformation into an unreported diaqua anhydrate, namely poly[diaqua(μ_2-benzene-1,2-dicarboxylato-κ^2O^1:O^2)(μ_2-4,4′-bipyridine-κ^2N:N')-cobalt(II)], $[Co(C_8H_4O_4)(C_{10}H_8N_2)(H_2O)_2]_n$, (II*a*). The structural change consists of the loss of the two solvent water molecules linking the original two-dimensional covalent substructures which are the 'main frame' of the monoclinic $P2/n$ hydrate (strictly preserved during the transformation), with further reaccommodation of the latter. The anhydrate organizes itself in the orthorhombic system (space group $Pmn2_1$) in a disordered fashion, where the space-group-symmetry restrictions are achieved only in a statistical sense, with mirror-related two-dimensional planar substructures, mirrored in a plane perpendicular to [100]. Thus, the asymmetric unit in the refined model is composed of two superimposed mirror-related 'ghosts' of half-occupancy each. Similarities and differences with the parent dihydrate and some other related structures in the literature are discussed.

Keywords: crystal structure; topotactic dehydration; disorder; 'average' mirror plane; robust two-dimensional substructure.

1. Introduction

Our group has studied a family of Co^{II} complexes of general formula $[Co(pht)_{n1}(bpy)_{n2}(H_2O)_{n3}]\cdot(H_2O)_{n4}$ (where pht is phthalate and bpy is 4,4′-bipyridine), and which we shall represent for simplicity by the shorthand subindices notation $n1$:$n2$:$n3$:($n4$). The system aroused our interest due to its elusiveness, the final formulation of these compounds being extremely sensitive to the synthetic conditions.

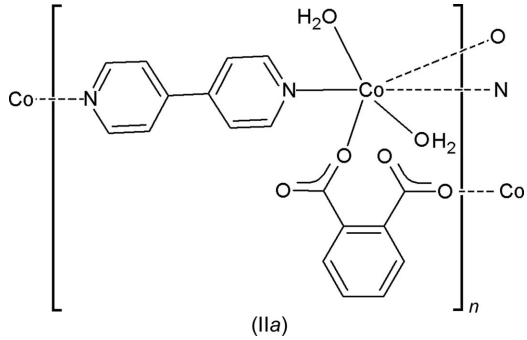

(II*a*)

Thermal treatment of some members of the family [in particular, the 1:1:1:(3) compound, (I) (Harvey *et al.*, 2014), and the 1:1:2:(2) compound, (II) (Köferstein & Robl, 2007)], as either powdered samples or single crystals, showed a number of similar features. Indeed, both (I) and (II) started as pale-rose hydrated materials and both transformed into deep-purple dehydrated products. The first mass loss detected in thermogravimetric analysis (TGA) studies agreed with the loss of the solvent water molecules in both cases, *viz.* three molecules per formula for (I) at 375–405 K, giving (I*a*), and two molecules per formula for (II) at *ca* 395–415 K, yielding (II*a*). Although (I*a*) showed a rather poor crystallinity – as expected given the key structural role played by these water molecules in the building up of the structure of (I) – precluding any direct structural characterization (Harvey *et al.* 2014), experiments performed on individual single crystals of (II), carefully heated in a differential scanning calorimetry (DSC) apparatus up to the end of the first thermal peak, allowed us to conduct this first dehydration process in such a way that the obtained specimens were single crystals suitable for X-ray data collection and (with some effort, see *Experimental*, §2) structure determination of (II*a*). The results show that the (II*a*) specimens correspond to disordered crystals with a so far unreported anhydrate of composition 1:1:2:(0), *viz.* $[Co(pht)(bpy)(H_2O)_2]_n$, (II*a*), the structure of which is presented herein. A conspicuous feature of the structure is the extremely ordered fashion in which disorder is achieved, a fact which will be discussed below. The colour change due to dehydration is explained in terms of the change in the coordination environment of the Co^{II} cations.

2. Experimental

2.1. Synthesis and crystallization

The parent dihydrate, (II), was synthesized *via* a slightly modified version of the method reported by Köferstein & Robl (2007). An aqueous solution of 4,4′-bpy (31.2 mg, 0.2 mmol, 2 ml H_2O, T = 353 K) was added to an aqueous solution of $Co(NO_3)_2\cdot 6H_2O$ (29.1 mg, 0.1 mmol, 1 ml H_2O), and to the resulting mixture an aqueous solution of potassium

  doi:10.1107/S2053229614020427

hydrogen pthalate (20.4 mg, 0.1 mmol, 1 ml H_2O) was added. The whole system was kept for 5 d at 353 K and autogenous pressure in a Teflon-lined Parr digestion vessel. After cooling to room temperature at a rate of 5 K h^{-1}, pale-rose prismatic crystals were obtained, which were suitable for all subsequent experiments. Analysis for $C_{18}H_{20}CoN_2O_8$ found (calculated): C 48.3 (47.91), H 4.5 (4.47), N 6.1% (6.21%).

Differential scanning calorimetry (DSC) experiments on selected single crystals of (II) were conducted on a Shimadzu DSC-50 apparatus, at a heating rate of 5 K min^{-1} under an N_2 atmosphere, using aluminum pans. Thermogravimetric analysis (TGA) was performed under similar conditions using a Shimadzu TGA-51H thermobalance. Elemental analyses were carried out at the Servicio a Terceros of INQUIMAE on a Carlo Erba CHNS-O EA1108 analyser. Diffuse reflectance spectra of both (II) and (II*a*) were acquired on pressed samples (Na_2SO_4 diluted) on an Ocean Optics instrument (OOIBase32) with a 50 mm integrating sphere. Typical corrections were applied. The corrected reflectance value for a given sample was thus calculated as $R = (Sa - D)/(Ref - D)$, where Sa, Ref and D stand for the measured values for that sample, for the reference and in the dark, respectively. The K/S coefficient, where $K = (1 - R)^2$ and $S = 2R$, has been plotted against λ (Fig. 1). For (II), λ_{max} = 485 nm, and for the dehydration product (II*a*), λ_{max} = 536 nm

2.2. Refinement

Difficulties in the structure determination of (II*a*) initially suggested this to be a hopeless case of merohedral twinning (no splitting of the diffraction peaks in the CCD frames). Attempts to solve and refine the structure as a twin in the monoclinic space group *Pn* [subgroup of the parent structure (II), space group *P*2/*n*] were not successful. However, the problem was finally treated satisfactorily in the orthorhombic system (suggested by the cell metrics), space group $Pmn2_1$ (uniquely defined by the systematic extinctions), with a split model of two mirror-related images of 0.50 occupancy each.

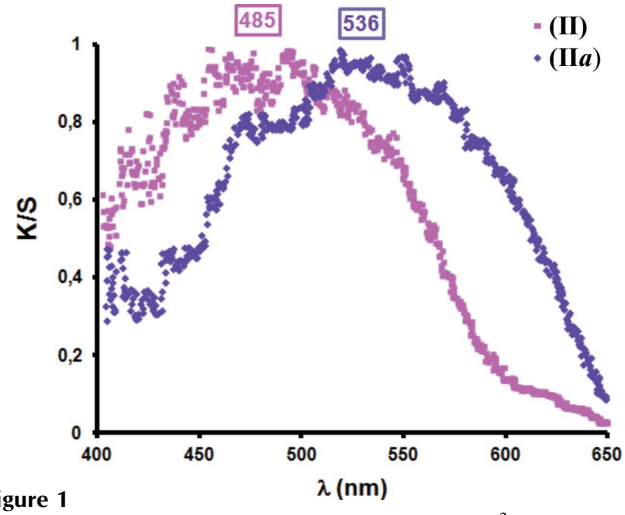

Figure 1
A plot of the K/S coefficient *versus* λ, where $K = (1 - R)^2$ and $S = 2R$. For (II), λ_{max} = 485 nm, and for the dehydration product (II*a*), λ_{max} = 536 nm.

Table 1
Experimental details.

Crystal data	
Chemical formula	$[Co(C_8H_4O_4)(C_{10}H_8N_2)(H_2O)_2]$
M_r	415.27
Crystal system, space group	Orthorhombic, $Pmn2_1$
Temperature (K)	294
a, *b*, *c* (Å)	7.575 (5), 11.410 (5), 10.106 (5)
V (Å^3)	873.5 (8)
Z	2
Radiation type	Mo *Kα*
μ (mm^{-1})	1.02
Crystal size (mm)	0.40 × 0.35 × 0.30
Data collection	
Diffractometer	Oxford Gemini S Ultra CCD area-detector diffractometer
Absorption correction	Multi-scan (*CrysAlis PRO*; Oxford Diffraction, 2009)
T_{min}, T_{max}	0.65, 0.74
No. of measured, independent and observed [$I > 2\sigma(I)$] reflections	6622, 1973, 1427
R_{int}	0.078
$(\sin\theta/\lambda)_{max}$ (Å^{-1})	0.687
Refinement	
$R[F^2 > 2\sigma(F^2)]$, $wR(F^2)$, *S*	0.064, 0.171, 1.00
No. of reflections	1973
No. of parameters	230
No. of restraints	435
H-atom treatment	H-atom parameters constrained
$\Delta\rho_{max}$, $\Delta\rho_{min}$ (e Å^{-3})	0.71, −0.42
Absolute structure	Flack (1983); refined as an inversion twin
Absolute structure parameter	0.33 (10)

Computer programs: *CrysAlis PRO* (Oxford Diffraction, 2009), *SHELXS97* (Sheldrick, 2008), *SHELXL2013* (Sheldrick, 2013), *SHELXTL* (Sheldrick, 2008), *SHELXL97* (Sheldrick, 2008) and *PLATON* (Spek, 2009).

Oddly, this (crystallographic) mirror plane exists only in a statistical sense, as the mirror-related entities are physically incompatible. Probably due to poor data quality (1427 observed reflections for 230 refined parameters), some strong *SHELXL2013* (Sheldrick, 2008) similarity restraints on distances (SAME 0.01, FLAT 0.01) and displacement factors (RIGU 0.001, SIMU 0.002) were needed to ensure a reasonable geometry.

H atoms attached to C atoms were added at their expected positions (C—H = 0.93 Å) and allowed to ride, with $U_{iso}(H) = 1.2U_{eq}(C)$. Water H atoms could obviously not be located and were not included in the model.

3. Results and discussion

Table 1 presents the full crystallographic data for (II*a*), while columns 2 and 3 in Table 2 display a few comparative values for the two topotactically related structures, (II) and (II*a*) (the remaining columns will be discussed later). Table 3, in turn, provides a comparison of the coordination distances for (II) and (II*a*).

The result of dehydration of the monoclinic (*P*2/*n*) structure, (II), is an orthorhombic anhydrate, (II*a*), which organizes itself in the space group $Pmn2_1$ in a highly disordered fashion where the space-group-symmetry restrictions are achieved only in a statistical sense. Fig. 2(*a*) presents a view of one of the two related halves in the asymmetric unit of (II*a*); the

Table 2
Comparative crystal data for (II)[a], (II*a*), (III)[b] and (IV)[c].

For (III) and (IV), the original cells were rotated so as to match those in (II) and (II*a*). The term 'mesh' refers to the parameters defining the planar 'unit cell' in the corresponding two-dimensional substructure. The mesh angle is given in square brackets.

	(II)	(II*a*)	(III)	(IV)
Chemical formula	$(C_{18}H_{16}CoN_2O_6{\cdot}2H_2O)_n$	$(C_{18}H_{16}CoN_2O_6)_n$	$(C_{18}H_{12}CoF_4N_2O_6)_n$	$(C_{20}H_{20}N_2O_6Zn)_n$
Crystal system, space group	Monoclinic, $P2/n$	Orthorhombic, $Pmn2_1$	Orthorhombic, $Pbnb$	Triclinic, $P\overline{1}$
a, b, c (Å)	7.6118 (9), 11.3569 (9), 10.8089 (9)	7.575 (5), 11.410 (5), 10.106 (5)	7.499 (1) 22.912 (1) 10.654 (1)	11.238 (5), 11.373 (5), 7.378 (3)
α, β, γ (°)	90, 92.276 (7), 90	90, 90, 90	90, 90, 90	94.771 (6), 105.027 (5), 90.253 (6)
V (Å^3)	933.65	873.5 (8)	1830.52	907.25
Z	2	2	4	2
Mesh (Å, °)	7.6118 (9), 11.3569 (9), [90]	7.575 (5), 11.410 (5), [90]	7.499 (1) 11.456 (1), [90]	11.238 (5), 11.373 (5), [90.253 (6)]
$d_{(002)}$ (Å)	5.400	5.053	5.327	3.549 (7.098)

References: (*a*) Köferstein & Robl (2007); (*b*) Hulvey *et al.* (2009); (*c*) Yang *et al.* (2010).

remaining half (not drawn, for clarity) is obtained by application of the crystallographic mirror plane normal to [100] and going through atoms Co1, N12, N22, C32 and C82 of the bpy spacer. Thus, the asymmetric unit in our model is composed of two superimposed mirror-related 'ghosts' of half-occupancy each. At this point, a first difference between (II) and (II*a*) can be highlighted. In the dihydrate, the molecule is strictly symmetric, threaded by a twofold axis passing through the cation and the bpy units, and the coordination environment around the Co^{II} cations is almost strictly octahedral. In the case of the anhydrate, this symmetry is lost and replaced by the 'twinning' mirror plane relating nonsymmetric entities.

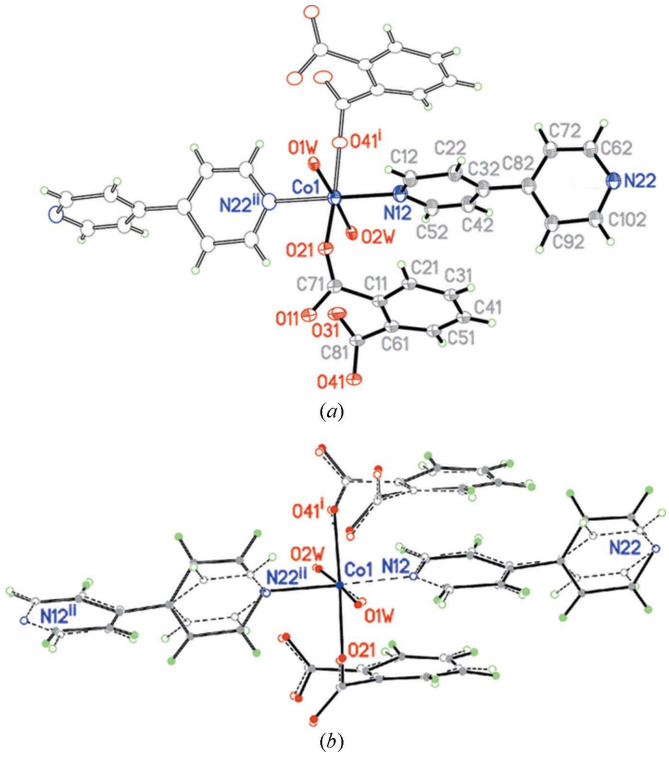

Figure 2
(*a*) A molecular view of one of the two related halves in the asymmetric unit of (II*a*), showing the atom-numbering scheme. Displacement ellipsoids are drawn at the 50% probability level. [Symmetry codes: (i) $x, y, z+1$; (ii) $x, y-1, z$]. (*b*) An overlapping view of the molecular units of (II*a*) and (II) (solid and broken lines, respectively).

This loss of symmetry is clearly assessed in Table 3, where the splitting [in (II*a*)] of the symmetry-related distances in (II) is apparent. In addition, a clear lengthening of $Co^{II}\cdots$bpy distances is observed in (II*a*), which could explain the colour change (a red shift of the likely *d*–*d* transition ascribed to a more distant position of both strong-field bpy ligands), as well as its increased intensity, likely due to the lack of symmetry. A further difference between the (otherwise strikingly similar) units is to be found in the conformation of the bridging bpy ligands, where individual pyridine units depart from a parallel disposition in a significantly different way, by 53.85 (9)° in (II) and 78.8 (8)° in (II*a*) (Fig. 2*b* shows a least-squares fit of both molecular environments of the Co^{II} cation, where similarities and differences can be clearly appreciated).

Similarities extend to the *leitmotif* in the crystal packing. This is the $[Co(pht)(bpy)(H_2O)_2]_n$ planar substructure shown in Fig. 3, in the form of a rectangular mesh having a –bpy– spacer along *b* and a –pht– one along *a*, joining Co^{II} cations at the corners. Fig. 4, in turn, shows two views of the stacking of these planar arrays for both compounds, now seen sideways, in projection along the bpy spacers. Fig. 4(*a*) shows the case of (II), with the solvent water molecules (with a grey background) located between the layers and fulfilling the role of active connectors. Fig. 4(*b*) presents the corresponding view in (II*a*), with narrow grey lines indicating the regions where these solvent molecules used to be. Comparison of the corresponding cell lengths in the two structures (Table 2) clearly reveals the geometric consequences of the loss of the solvent water molecules. The effect is almost nil along *b* (slight expansion < 0.5% along the bpy bridge) and *a* (slight

Table 3
Comparison of the Co coordination environments in dihydrate (II)[a] and anhydrate (II*a*).

(II)		(II*a*)	
Bond	Distance (Å)	Bond	Distance (Å)
Co—O2 (×2)	2.137 (2)	Co1—O21	2.176 (16)
		Co1—O41^{i}	2.022 (14)
Co—O*W*1 (×2)	2.127 (2)	Co1—O1*W*	2.051 (18)
		Co1—O2*W*	2.192 (19)
Co—N1	2.135 (3)	Co1—N12	2.171 (6)
Co—N2	2.149 (3)	Co1—N22^{ii}	2.202 (6)

Reference: (*a*) Köferstein & Robl (2007). Symmetry codes: (i) $x-1, y, z$; (ii) $-x, y-1, z$.

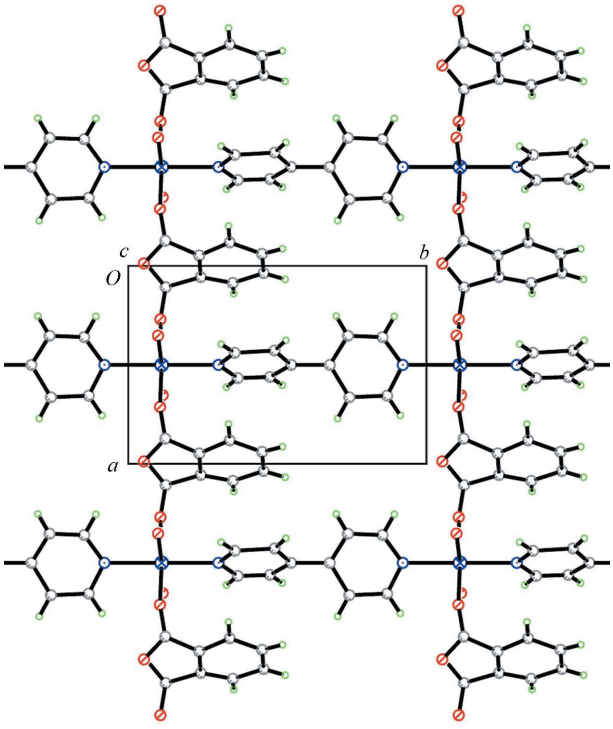

Figure 3
A packing view of (II*a*), projected along [001], showing one of the two-dimensional network structures.

contraction < 0.6% along the pht bridge) but significant along *c* [a noticeable contraction of ∼7% in the [001] direction and ∼8% in the (002) interplanar spacing]. The contracting effect along [001] is thus apparent.

The interplanar linkage in (II) is achieved through the intermediation of the solvent water molecules (Fig. 4*a*, grey zones), so their removal should introduce some instability to the resulting structure. The observed 8% interplanar shrinkage and a parallel in-plane reaccommodation, with a concomitant reshuffling of the contacts of the aqua molecules, tend to mediate this potential weakness. The interplanar hydrogen bonds to atom O11 in the dihydrate (Table 4, entries 1 and 4), basically developing the structure along *a*, are kept unperturbed upon dehydration, as expected from the discussion above, while the bonds originally involving the (now removed) solvent water molecule O3*W* (Table 4, entries 2 and 3) redirect to atom O31 and form new links to neighbouring planes, as presented in Table 5. Even though the water H atoms could not be included in the (II*a*) model, Table 5 presents short O···O contacts clearly ascribable to hydrogen bonds. Indeed, further heating at higher temperatures gave rise to noncrystalline products; the solid obtained from a crop of single crystals heated to *ca* 548 K (above the second mass loss in TGA) in a DSC apparatus turned out to be a Co:1:1:1(0) anhydrate after elemental analysis [analysis for $C_{18}H_{16}CoN_2O_6$ found (calculated): C 55.3 (54.42), H 3.6 (3.55), N 6.8% (7.05%)].

On the other hand, for this reshuffling yielding (II*a*) to be feasible, neighbouring planes have to reaccommodate parallel to each other, and the way in which this happens is clearly disclosed from Fig. 5, where [001] projections of the distribution of Co^{II} cations for both structures are presented. In structure (II), cations in neighbouring layers (shown in blue and cyan, respectively) alternate in a nearly centred structure, with similar Co···Co distances between nearest neighbours in vicinal planes [8.193 (2) and 9.225 (2) Å]. However, with this

Table 4
Hydrogen-bond geometry (Å, °) for (II).

D—H···*A*	*D*—H	H···*A*	*D*···*A*	*D*—H···*A*
O1*W*—H1*WA*···O11^{i}	0.75 (3)	1.96 (3)	2.703 (2)	179 (6)
O1*W*—H1*WB*···O3*W*^{ii}	0.84 (3)	1.92 (3)	2.715 (3)	160 (3)
O3*W*—H3*WA*···O21^{ii}	0.92 (3)	1.98 (3)	2.810 (3)	149 (3)
O3*W*—H3*WB*···O11	0.83 (3)	2.02 (3)	2.834 (3)	166 (4)

Symmetry codes: (i) $x+1, y, z$; (ii) $-x, -y+1, -z+2$.

Table 5
Short O_{water}···O contacts (Å) for (II*a*).

O1*W*···O11^{i}	2.80 (3)	O2*W*···O11^{iv}	2.78 (3)
O1*W*···O31^{iii}	2.74 (3)	O2*W*···O31	2.63 (3)

Symmetry codes: (i) $x-1, y, z$; (iii) $x-\frac{1}{2}, -y, z+\frac{1}{2}$; (iv) $x-\frac{1}{2}, -y, z-\frac{1}{2}$.

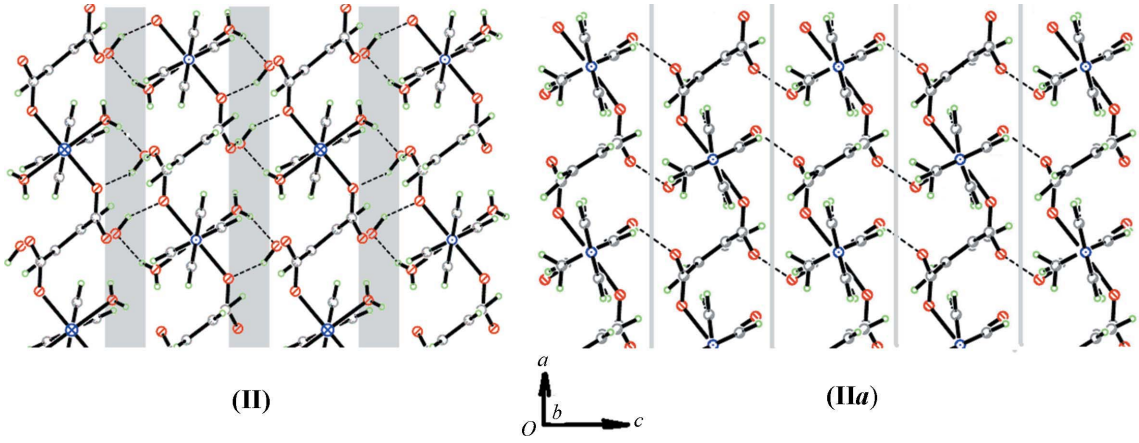

Figure 4
Comparative packing views of (II) and (II*a*), projected along [010]. For (II), details of the hydrogen bonds (broken lines) are presented in Table 3. For (II*a*), details of the O···O contacts that can be interpreted as hydrogen bonds are presented in Table 4.

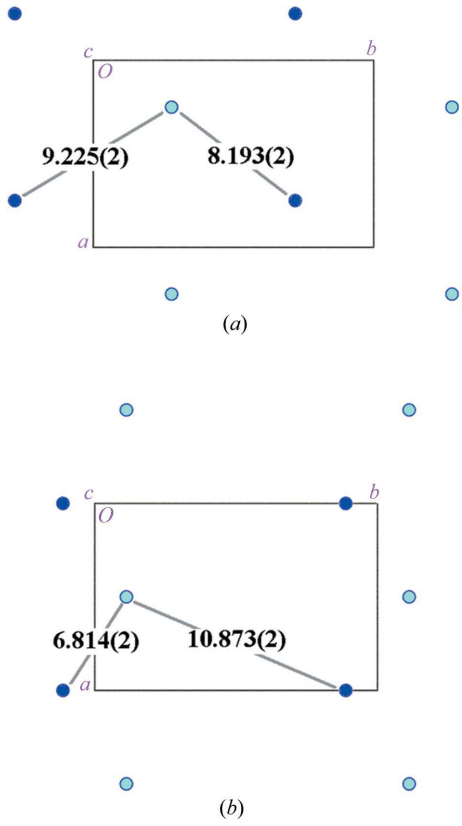

Figure 5
Comparative packing views of (*a*) (II) and (*b*) (II*a*), projected along [001], showing the different cation dispositions. Distances are in Ångströms (Å).

molecular disposition, the shortest O···O contact which the coordinated water O atom could make to a neighbouring O atom from a parallel plane would be O1···O3($-x$, $-y+1$, $-z+2$) of 4.940 (4) Å. Thus, a parallel shift between planes would be in force to allow for the shorter approach reported in Table 5 to take place. Fig. 5(*b*) shows this to be the case, with a significant differentiation of Co···Co distances between adjacent planes [*viz.* 6.814 (2) and 10.873 (2) Å], suggesting some kind of alignment of coordination polyhedra along *c*.

Looking for related structures in the literature, we found two compounds of the same 1:1:2:(0) type and similar topology (Table 2, columns 4 and 5). The first is a Co^{II} complex with tetrafluorophthalate instead of pht, *viz.* *catena*-[diaqua(μ_2-4,4′-bipyridine)(μ_2-tetrafluorophthalato)cobalt], (III) [Cambridge Structural Database (CSD; Version 5.35; Allen, 2002) refcode QUKQOD (Hulvey *et al.*, 2009)]. In spite of having different space groups, (III) and (II*a*) are very nearly isostructural, with the only difference for (III) being a cell doubling along the direction of the bpy bridge. The mesh size and geometry are basically unaltered (Table 2), and the replacement of H for F in the phenyl ring has an expansion effect in the interplanar (002) spacing (Table 2). Irrespective of this, the hydrogen-bonding scheme is the same as that described for (II*a*), with one intraplanar hydrogen bond along *a* and a second one linking planes along *c*.

The second compound selected for comparison includes Zn^{II} as the cation and 1,2-phenylenediacetate instead of pht, *viz.* *catena*-[diaqua(μ_2-4,4′-bipyridine)(μ_2-2,2′-phenylenediacetato)zinc], (IV) (CSD refcode CUYHEK; Yang *et al.*, 2010). The compound presents a two-dimensional substructure topologically identical to that in (II*a*), with an expected geometric expansion along *a* (Table 2) due to the larger CH_2CO_2 bridging arms compared with CO_2 in (II*a*). However, the way in which the linkage between planes takes place deserves a detailed analysis. Even though the interaction scheme is the same as usual (one 'in-plane' and one 'interplane' hydrogen bond), the longer arms allow for a more expanded disposition of the carboxylate acceptor along the *c* direction. Thus, the interaction ends up taking place between planar arrays separated by exactly one whole *c* translation [$d_{(001)}$ = 7.098 Å], much larger than those discussed previously for (II), (II*a*) and (III). The result is that the (now very large) voids appearing between planes in this hydrogen-bonded three-dimensional substructure are filled by a similar interpenetrating substructure with no relevant interactions with the former one (except second-order contacts). The shift parallel to the planes between these two substructures is *ca* *a*/2, *b*/2, so that the interplanar interaction linking the planes in one of them goes exactly through the unoccupied centre of a mesh in the other.

Summarizing, the present analysis suggests that the two-dimensional array found in (II*a*) is certainly not exclusive and appears to be a robust building block, accepting a variety of ligands and cations. Even though its geometry (as a right-angled mesh) seems to be rather stiff, it can accept a number of interplanar interactions, all of them promoted by the aqua H atoms, either as direct connectors [as in (III) and (IV)] or as intermediate linkers [as in (II)].

The authors acknowledge ANPCyT (project No. PME 2006-01113) for the purchase of the Oxford Gemini CCD diffractometer. FDC is a member of the research staff of CONICET.

References

Allen, F. H. (2002). *Acta Cryst.* B**58**, 380–388.
Flack, H. D. (1983). *Acta Cryst.* A**39**, 876–881.
Harvey, M. A., Suarez, S., Doctorovich, F., Cukiernik, F. D. & Baggio, R. (2014). *Acta Cryst.* C**70**, 440–444.
Hulvey, Z., Ayala, E. & Cheetham, A. K. (2009). *Z. Anorg. Allg. Chem.* **635**, 1753–1757.
Köferstein, R. & Robl, C. (2007). *Z. Anorg. Allg. Chem.* **633**, 1127–1130.
Oxford Diffraction (2009). *CrysAlis PRO*. Oxford Diffraction Ltd, Yarnton, Oxfordshire, England.
Sheldrick, G. M. (2008). *Acta Cryst.* A**64**, 112–122.
Sheldrick, G. M. (2013). *SHELXL2013*. University of Göttingen, Germany.
Spek, A. L. (2009). *Acta Cryst.* D**65**, 148–155.
Yang, G.-P., Wang, Y.-Y., Zhang, W.-H., Fu, A.-Y., Liu, R.-T., Lermontova, E. K. & Shi, Q.-Z. (2010). *CrystEngComm*, **12**, 1509–1517.

supporting information

Acta Cryst. (2014). C**70**, 978-982 [doi:10.1107/S2053229614020427]

The topotactic dehydration of monoclinic $\{[Co(pht)(bpy)(H_2O)_2]\cdot 2H_2O\}_n$ into orthorhombic $[Co(pht)(bpy)(H_2O)_2]_n$ (pht is phthalate and bpy is 4,4′-bipyridine)

Miguel Angel Harvey, Sebastián Suarez, Fabio D. Cukiernik and Ricardo Baggio

Computing details

Data collection: *CrysAlis PRO* (Oxford Diffraction, 2009); cell refinement: *CrysAlis PRO* (Oxford Diffraction, 2009); data reduction: *CrysAlis PRO* (Oxford Diffraction, 2009); program(s) used to solve structure: *SHELXS97* (Sheldrick, 2008); program(s) used to refine structure: *SHELXL2013* (Sheldrick, 2013); molecular graphics: *SHELXTL* (Sheldrick, 2008); software used to prepare material for publication: *SHELXL97* (Sheldrick, 2008) and *PLATON* (Spek, 2009).

Poly[diaqua(μ_2-benzene-1,2-dicarboxylato-κ^2O^1:O^2)(μ_2-4,4′-bipyridine-κ^2N:N')cobalt(II)]

Crystal data

$[Co(C_8H_4O_4)(C_{10}H_8N_2)(H_2O)_2]$
M_r = 415.27
Orthorhombic, $Pmn2_1$
a = 7.575 (5) Å
b = 11.410 (5) Å
c = 10.106 (5) Å
V = 873.5 (8) Å^3
Z = 2
$F(000)$ = 426
D_x = 1.579 Mg m^{-3}
Mo $K\alpha$ radiation, λ = 0.71073 Å
Cell parameters from 902 reflections
θ = 3.8–24.2°
μ = 1.02 mm^{-1}
T = 294 K
Prism, violet
0.40 × 0.35 × 0.30 mm

Data collection

Oxford Gemini S Ultra CCD area-detector diffractometer
Radiation source: fine-focus sealed tube
Graphite monochromator
ω scans, thick slices
Absorption correction: multi-scan (*CrysAlis PRO*; Oxford Diffraction, 2009)
T_{min} = 0.65, T_{max} = 0.74
6622 measured reflections
1973 independent reflections
1427 reflections with $I > 2\sigma(I)$
R_{int} = 0.078
θ_{max} = 29.2°, θ_{min} = 3.8°
h = −10→10
k = −13→14
l = −12→12

Refinement

Refinement on F^2
Least-squares matrix: full
$R[F^2 > 2\sigma(F^2)]$ = 0.064
$wR(F^2)$ = 0.171
S = 1.00
1973 reflections
230 parameters
435 restraints
Hydrogen site location: inferred from neighbouring sites
H-atom parameters constrained
$w = 1/[\sigma^2(F_o^2) + (0.0843P)^2 + 0.948P]$ where $P = (F_o^2 + 2F_c^2)/3$
$(\Delta/\sigma)_{max} < 0.001$
$\Delta\rho_{max}$ = 0.71 e Å^{-3}
$\Delta\rho_{min}$ = −0.42 e Å^{-3}

Absolute structure: Flack (1983); refined as an inversion twin

Absolute structure parameter: 0.33 (10)

Special details

Geometry. All e.s.d.'s (except the e.s.d. in the dihedral angle between two l.s. planes) are estimated using the full covariance matrix. The cell e.s.d.'s are taken into account individually in the estimation of e.s.d.'s in distances, angles and torsion angles; correlations between e.s.d.'s in cell parameters are only used when they are defined by crystal symmetry. An approximate (isotropic) treatment of cell e.s.d.'s is used for estimating e.s.d.'s involving l.s. planes.

Refinement. Refined as a 2-component inversion twin.

Fractional atomic coordinates and isotropic or equivalent isotropic displacement parameters (Å²)

	x	*y*	*z*	U_{iso}*/U_{eq}	Occ. (<1)
Co1	0.5000	0.11228 (9)	0.5146 (9)	0.0314 (4)	
N12	0.5000	0.3025 (5)	0.5173 (16)	0.0243 (10)	
N22	0.5000	0.9194 (5)	0.5078 (13)	0.0280 (12)	
C32	0.5000	0.5468 (6)	0.5227 (16)	0.0253 (11)	
C82	0.5000	0.6755 (6)	0.517 (3)	0.0261 (11)	
O11	1.016 (3)	0.0518 (10)	0.6642 (17)	0.037 (2)	0.5
O21	0.7300 (18)	0.1045 (11)	0.643 (2)	0.0317 (17)	0.5
O31	1.004 (4)	0.0623 (10)	0.3469 (15)	0.034 (2)	0.5
O41	1.2889 (15)	0.1105 (12)	0.392 (2)	0.0278 (18)	0.5
C11	0.9523 (16)	0.2410 (11)	0.5716 (15)	0.0307 (12)	0.5
C21	0.8999 (15)	0.3482 (13)	0.6218 (12)	0.0311 (14)	0.5
H21A	0.8290	0.3506	0.6969	0.037*	0.5
C31	0.951 (2)	0.4521 (10)	0.5622 (17)	0.0311 (15)	0.5
H31A	0.9153	0.5232	0.5983	0.037*	0.5
C41	1.055 (2)	0.4513 (12)	0.4496 (17)	0.0308 (15)	0.5
H41A	1.0880	0.5209	0.4086	0.037*	0.5
C51	1.1087 (16)	0.3438 (13)	0.3996 (13)	0.0305 (14)	0.5
H51A	1.1793	0.3411	0.3244	0.037*	0.5
C61	1.0579 (17)	0.2407 (10)	0.4607 (15)	0.0297 (12)	0.5
C71	0.8943 (16)	0.1245 (14)	0.637 (2)	0.0317 (14)	0.5
C81	1.1236 (17)	0.1252 (14)	0.397 (2)	0.0289 (15)	0.5
C12	0.4313 (10)	0.3601 (11)	0.6194 (14)	0.0253 (13)	0.5
H12A	0.3891	0.3172	0.6910	0.030*	0.5
C22	0.4198 (19)	0.4815 (10)	0.6237 (15)	0.0255 (13)	0.5
H22A	0.3602	0.5188	0.6923	0.031*	0.5
C42	0.5555 (17)	0.4851 (10)	0.4102 (14)	0.0255 (13)	0.5
H42A	0.5891	0.5249	0.3339	0.031*	0.5
C52	0.5595 (11)	0.3633 (10)	0.4147 (14)	0.0253 (13)	0.5
H52A	0.6057	0.3228	0.3428	0.030*	0.5
C62	0.3551 (12)	0.8591 (8)	0.4773 (10)	0.0284 (14)	0.5
H62A	0.2517	0.9000	0.4596	0.034*	0.5
C72	0.3522 (15)	0.7377 (8)	0.4709 (18)	0.0275 (14)	0.5
H72A	0.2547	0.6983	0.4370	0.033*	0.5
C92	0.6590 (12)	0.7397 (7)	0.529 (2)	0.0263 (14)	0.5
H92A	0.7672	0.7015	0.5348	0.032*	0.5

C102	0.6492 (11)	0.8614 (8)	0.5333 (12)	0.0276 (14)	0.5
H10A	0.7502	0.9038	0.5544	0.033*	0.5
O1W	0.357 (2)	0.1045 (12)	0.687 (2)	0.027 (3)	0.5
O2W	0.659 (3)	0.1106 (14)	0.333 (2)	0.034 (4)	0.5

Atomic displacement parameters (Å²)

	U^{11}	U^{22}	U^{33}	U^{12}	U^{13}	U^{23}
Co1	0.0241 (6)	0.0146 (5)	0.0555 (8)	0.000	0.000	0.0036 (13)
N12	0.023 (2)	0.0188 (18)	0.031 (2)	0.000	0.000	0.003 (3)
N22	0.029 (2)	0.021 (2)	0.035 (3)	0.000	0.000	0.004 (3)
C32	0.025 (2)	0.0201 (18)	0.031 (2)	0.000	0.000	0.003 (3)
C82	0.027 (2)	0.0206 (18)	0.030 (2)	0.000	0.000	0.004 (3)
O11	0.021 (4)	0.027 (4)	0.064 (5)	0.009 (4)	0.000 (4)	0.006 (4)
O21	0.020 (3)	0.021 (3)	0.054 (3)	0.006 (3)	0.000 (2)	−0.001 (4)
O31	0.012 (3)	0.031 (4)	0.059 (5)	0.006 (4)	−0.004 (4)	−0.010 (4)
O41	0.012 (3)	0.021 (3)	0.049 (4)	0.007 (3)	−0.008 (3)	0.001 (4)
C11	0.018 (2)	0.022 (2)	0.052 (2)	0.006 (3)	−0.0040 (18)	0.000 (4)
C21	0.019 (3)	0.022 (2)	0.052 (3)	0.007 (3)	−0.005 (2)	0.000 (4)
C31	0.020 (3)	0.022 (2)	0.052 (3)	0.006 (3)	−0.007 (2)	0.000 (4)
C41	0.019 (3)	0.022 (2)	0.051 (3)	0.005 (3)	−0.008 (2)	0.001 (4)
C51	0.018 (3)	0.022 (2)	0.052 (3)	0.005 (3)	−0.006 (2)	0.001 (4)
C61	0.016 (2)	0.022 (2)	0.051 (3)	0.007 (3)	−0.0058 (19)	0.000 (4)
C71	0.019 (3)	0.022 (2)	0.054 (3)	0.006 (3)	−0.001 (2)	0.000 (4)
C81	0.013 (3)	0.023 (3)	0.051 (3)	0.007 (3)	−0.007 (2)	0.000 (4)
C12	0.025 (2)	0.020 (2)	0.032 (3)	−0.0008 (17)	0.0008 (17)	0.003 (3)
C22	0.025 (2)	0.020 (2)	0.032 (3)	−0.0004 (17)	0.0007 (17)	0.003 (3)
C42	0.025 (3)	0.020 (2)	0.032 (3)	−0.0001 (17)	0.0003 (17)	0.003 (3)
C52	0.024 (2)	0.020 (2)	0.032 (3)	0.0003 (17)	0.0004 (16)	0.003 (3)
C62	0.029 (2)	0.021 (2)	0.035 (3)	−0.0005 (15)	−0.0011 (17)	0.005 (3)
C72	0.028 (2)	0.021 (2)	0.033 (3)	−0.0004 (15)	−0.0012 (17)	0.005 (3)
C92	0.027 (2)	0.021 (2)	0.031 (3)	0.0001 (14)	−0.0003 (17)	0.003 (3)
C102	0.029 (2)	0.021 (2)	0.033 (3)	0.0004 (14)	−0.0004 (17)	0.003 (3)
O1W	0.016 (5)	0.017 (7)	0.050 (4)	−0.004 (4)	−0.004 (4)	0.002 (4)
O2W	0.024 (6)	0.025 (8)	0.053 (4)	0.001 (5)	0.001 (4)	0.004 (4)

Geometric parameters (Å, º)

Co1—O41^{i}	2.022 (14)	C11—C71	1.550 (12)
Co1—O1W	2.051 (18)	C21—C31	1.385 (9)
Co1—N12	2.171 (6)	C21—H21A	0.9300
Co1—O21	2.176 (16)	C31—C41	1.384 (9)
Co1—O2W	2.192 (19)	C31—H31A	0.9300
Co1—N22^{ii}	2.202 (6)	C41—C51	1.387 (9)
N12—C52	1.326 (9)	C41—H41A	0.9300
N12—C12	1.329 (9)	C51—C61	1.384 (9)
N22—C62	1.331 (9)	C51—H51A	0.9300
N22—C102	1.335 (8)	C61—C81	1.547 (12)

N22—Co1^{iii}	2.202 (6)	C12—C22	1.389 (10)
C32—C42	1.401 (10)	C12—H12A	0.9300
C32—C22	1.402 (10)	C22—H22A	0.9300
C32—C82	1.470 (10)	C42—C52	1.391 (10)
C82—C72	1.404 (10)	C42—H42A	0.9300
C82—C92	1.415 (9)	C52—H52A	0.9300
O11—C71	1.267 (13)	C62—C72	1.387 (10)
O21—C71	1.267 (11)	C62—H62A	0.9300
O31—C81	1.265 (14)	C72—H72A	0.9300
O41—C81	1.264 (11)	C92—C102	1.391 (10)
O41—Co1^{iv}	2.022 (14)	C92—H92A	0.9300
C11—C61	1.377 (9)	C102—H10A	0.9300
C11—C21	1.382 (9)		

O41^{i}—Co1—N12	91.0 (5)	C61—C51—C41	120.5 (8)
O1W—Co1—N12	91.9 (6)	C61—C51—H51A	119.7
O41^{i}—Co1—O21	176.9 (4)	C41—C51—H51A	119.7
N12—Co1—O21	91.9 (4)	C11—C61—C51	121.5 (9)
O1W—Co1—O2W	176.7 (6)	C11—C61—C81	121.8 (15)
N12—Co1—O2W	91.1 (6)	C51—C61—C81	116.8 (15)
O41^{i}—Co1—N22^{ii}	88.3 (5)	O11—C71—O21	125.7 (15)
O1W—Co1—N22^{ii}	89.0 (6)	O11—C71—C11	116.7 (11)
N12—Co1—N22^{ii}	178.9 (7)	O21—C71—C11	116.9 (11)
O21—Co1—N22^{ii}	88.7 (4)	O41—C81—O31	128.3 (19)
O2W—Co1—N22^{ii}	88.0 (6)	O41—C81—C61	116.6 (12)
C52—N12—C12	118.8 (7)	O31—C81—C61	114.7 (12)
C52—N12—Co1	120.9 (9)	N12—C12—C22	122.8 (7)
C12—N12—Co1	120.2 (9)	N12—C12—H12A	118.6
C62—N22—C102	119.1 (6)	C22—C12—H12A	118.6
C62—N22—Co1^{iii}	121.6 (5)	C12—C22—C32	118.7 (7)
C102—N22—Co1^{iii}	119.3 (5)	C12—C22—H22A	120.7
C42—C32—C22	117.0 (7)	C32—C22—H22A	120.7
C42—C32—C82	118.0 (13)	C52—C42—C32	118.8 (7)
C22—C32—C82	124.0 (12)	C52—C42—H42A	120.6
C72—C82—C92	116.5 (8)	C32—C42—H42A	120.6
C72—C82—C32	121.2 (7)	N12—C52—C42	122.8 (7)
C92—C82—C32	120.9 (4)	N12—C52—H52A	118.6
C71—O21—Co1	138.7 (17)	C42—C52—H52A	118.6
C81—O41—Co1^{iv}	139.2 (18)	N22—C62—C72	122.7 (7)
C61—C11—C21	117.9 (11)	N22—C62—H62A	118.6
C61—C11—C71	120.7 (15)	C72—C62—H62A	118.6
C21—C11—C71	121.4 (14)	C62—C72—C82	118.4 (7)
C11—C21—C31	121.1 (8)	C62—C72—H72A	120.8
C11—C21—H21A	119.4	C82—C72—H72A	120.8
C31—C21—H21A	119.4	C102—C92—C82	118.3 (6)
C41—C31—C21	120.8 (10)	C102—C92—H92A	120.9
C41—C31—H31A	119.6	C82—C92—H92A	120.9
C21—C31—H31A	119.6	N22—C102—C92	122.3 (7)

C31—C41—C51	118.2 (11)	N22—C102—H10A	118.8
C31—C41—H41A	120.9	C92—C102—H10A	118.8
C51—C41—H41A	120.9		

Symmetry codes: (i) $x-1, y, z$; (ii) $x, y-1, z$; (iii) $x, y+1, z$; (iv) $x+1, y, z$.